Synthesis, Electrochemical, and Photophysical Study of Covalently Linked Porphyrin Dimers with Two Different Macrocycles

Karl M. Kadish,*,† Ning Guo,† Eric Van Caemelbecke,† Antonella Froiio,‡ Roberto Paolesse,*,‡ Donato Monti,‡ Pietro Tagliatesta,*,‡ Tristano Boschi,‡ Luca Prodi,*,§ Fabrizio Bolletta,§ and Nelsi Zaccheroni§

Department of Chemistry, University of Houston, Houston, Texas 77204-5641, Dipartimento di Scienze e Tecnologie Chimiche, Università di Roma "Tor Vergata", 00133 Roma, Italy, and Dipartimento di Chimica "G. Ciamician", Università di Bologna, 40126 Bologna, Italy

Received November 14, 1997

Four unsymmetrical covalently linked porphyrin dimers were synthesized, and their electrochemical, spectroelectrochemical, and/or photophysical properties were examined. The investigated compounds are represented as M[*p*-(TPP-DEHMP)]M and M[*m*-(TPP-DEHMP)]M (M = H_2, Zn), where *p*-(TPP-DEHMP) is the tetraanion of 1-[5-(10,15,20-triphenylporphyrinyl)]-4-[10-(2,18-diethyl-3,7,8,12,13,17-hexamethylporphyrinyl)]benzene and *m*-(TPP-DEHMP) is the tetraanion of 1-[5-(10,15,20-triphenylporphyrinyl)]-3-[10-(2,18-diethyl-3,7,8,12,13,17-hexamethylporphyrinyl)]benzene. The oxidation and reduction potentials of Zn[*p*-(TPP-DEHMP)]Zn are virtually identical to combined oxidation and reduction potentials of (TPP)Zn and (OEP)Zn, i.e., cyclic voltammograms of the heterodimers resemble those of the superposed monomeric units under the same experimental conditions. The UV−visible spectra of neutral, singly oxidized, and/or singly reduced Zn[*p*-(TPP-DEHMP)]Zn also resemble superposed spectra of the respective neutral, oxidized, or reduced monomeric (TPP)Zn and (OEP)Zn derivatives. Hence, both the electrochemical and spectroelectrochemical data suggest that there is little electronic interaction between the two subunits of the heterodimers in their neutral, singly oxidized, or singly reduced forms. The photophysical properties of four related homoleptic dimers, M[*p*-(TPP-TPP)]M and M[*m*-(TPP-TPP)]M, where M = H_2 or Zn, *p*-(TPP-TPP) = the tetraanion of 1, 4-bis[5′-(10′,15′,20′-triphenylporphyrinyl)]benzene, and *m*-(TPP-TPP) = the tetraanion of 1,3-bis[5′-(10′,15′,20′-triphenylporphyrinyl)]benzene, were also examined, and their data were compared to the data for the above heteroleptic dimers. Irradiation of H_2[*p*-(TPP-DEHMP)]H_2 and M[*m*-(TPP-DEHMP)]M (M = H_2, Zn) with excitation wavelengths in the visible spectrum of the DEHMP subunit, results in an efficient energy transfer between the DEHMP and TPP moieties. Calculated energy transfer rate constants agree well with the experimental data and suggest that the energy transfer processes are best described by a Föster mechanism. H_2[*p*-(TPP-DEHMP)]H_2 and H_2[*m*-(TPP-DEHMP)]H_2 thus demonstrate highly efficient and directional energy transfer processes *rather* than charge separation between the two subunits after irradiation.

Introduction

The photosynthetic reaction center of *Rhodopseudomonas viridis*[1] and *Rhodobacter sphaeroides*[1] consists of different tetrapyrroles held by the protein matrix in a well-organized tridimensional structure. Furthermore, crystallographic studies performed on the light-harvesting antenna systems of bacteria and green plants, also if at lower resolution, indicate an even more complex arrangement with a large number of chromophores embedded by self-assembling proteins.[2]

The basic conversion and storage processes of solar energy in bacteria and green plants involves first the collection of sunlight by a light-harvesting antenna system followed by an energy funnel to the reaction center through rapid and efficient transfer processes between chromophores. In the reaction center, an electron-transfer process starts from a primary electron donor constituted by two bacteriochlorophylls held in close proximity (the so-called "special pair") and then the electron is transferred along an energy gradient to the final acceptor with the formation of a charge-separated state.[3] A detailed knowledge of all factors influencing these processes has yet to be achieved and many issues are still unclear. Spectroscopic and theoretical studies of the photosynthetic processes are difficult to acquire directly on natural systems because of their complexity and a useful approach has been the development of simple synthetic models: such molecules provide the advantage to mimic natural processes without the complex structure of the protein scaffolding.[4]

Porphyrin dimers or oligomers are good photosynthetic models in that the geometry, distance, and/or angle between the porphyrin moieties strongly influence the efficiency of the

* Corresponding authors.
† University of Houston.
‡ Università di Roma.
§ Università di Bologna.

(1) (a) Deisenhofer, J.; Epp, O.; Miki, K.; Huber, R.; Michel, H. *J. Mol. Biol.* **1984**, *180*, 385. (b) Deisenhofer, J.; Epp, O.; Miki, K.; Huber, R.; Michel, H. *Nature* **1985**, *318*, 618. (c) Deisenhofer, J.; Michel, H. *Science* **1989**, *245*, 1463. (d) El-Kabbani, O.; Chang, C.-H.; Tiede, D.; Norris, J.; Schiffer, M. *Biochemistry* **1991**, *30*, 5361.
(2) (a) Kühlbrandt, W.; Da Neng, W.; Fujiyoshi, Y. *Nature* **1994**, *367*, 614. (b) McDermott, G.; Prince, S. M.; Freer, A. A.; Hawthornthwaite-Lawless, A. M.; Papiz, M. Z.; Cogdell, R. J.; Isaacs, N. W. *Nature* **1995**, *374*, 517.
(3) (a) Chang, C.-K.; Tiede, D. M.; Tang, J.; Norris, J. R.; Schiffer, M. *FEBS Lett.* **1986**, 205, 82. (b) Gust, D.; Moore, T. A. *Topics Curr. Chem.* **1991**, *159*, 103. (c) Gust, D.; Moore, T. A.; Moore, A. L. *Acc. Chem. Res.* **1993**, *26*, 198.
(4) (a) Wasielewski, M. R. *Chem. Rev.* **1992**, *92*, 435. (b) Kurreck, H.; Huber, M. *Angew. Chem. Int. Ed. Engl.* **1995**, *34*, 849.

S0020-1669(97)01443-2 CCC: $15.00
Published on Web 04/28/1998

photophysical processes.[4,5] Irradiation of a porphyrin dimer can be followed by two different processes between the subunits: an energy transfer, an electron transfer, or a combination of both processes. The specific mechanism will depend on the type of dimer, i.e., homoleptic or heteroleptic, and the type of interaction between the two moieties of the dimeric unit.

A charge separation between chromophores is not observed in light-harvesting antenna system of bacteria and green plants which provides energy to the special pair in the reaction center, and it was therefore of interest to synthesize porphyrin dyads in which energy transfer but not electron transfer would occur between the two subunits immediately after irradiation.[5] A knowledge of the deactivation mechanism and the direction of energy transfer following irradiation of such compounds should provide information as to the nature of the chromophores and their role in the photochemical properties of natural antenna systems.

Most synthetic models for photosynthesis contain two covalently linked porphyrins which are attached to each other by one or more bridging groups such as phenyls, biphenyls, aromatic heterocycles, alkenes, or alkynes.[6] Supramolecular assemblies held together by noncovalent forces such as hydrogen bonding or van der Waals interactions have also been synthesized as model compounds for photosynthetic processes in natural systems and show that photoinduced energy transfer can occur between two moieties of the dimers which are not linked by a bridging group.[7] However, the fact that the porphyrins used in these supramolecular assemblies possess two identical macrocycles does not allow for a selective excitation nor an elucidation of the energy transfer pathway upon irradiation.

The direction of photoinduced energy transfer has been generally induced in porphyrin model compounds by selective metalation and there are relatively few examples in the literature of directional energy transfer involving free base porphyrins; these include a tetraarylporphyrin which is covalently linked to a pyropheophorbide,[6u] a porphyrin−sapphyrin heterodimer which is held together by hydrogen bonds,[7c] a covalently linked chlorophyll−porphyrin heterodimer[6o] and several heteroporphyrin dyads with amide linkages.[6v] Unsymmetrical porphyrin dimers are potential models for photosynthetic energy transfer and should provide information about the role played by the electronic properties of the porphyrins in the yield and direction of energy transfer. This point is examined in the present study which reports the photophysical, electrochemical and spectroscopic properties of synthetic covalently linked porphyrin dimers containing two different macrocycles.[8]

One of the macrocycles is a tetraphenylporphyrin unit (TPP) and the other an alkylporphyrin unit (DEHMP). The two macrocycles possess different electronic properties[9] of their π ring systems which suggests that they could be selectively irradiated and the energy transfer pathway elucidated after photoexcitation with a suitable wavelength. The investigated compounds are represented as M[*p*-(TPP-DEHMP)]M and M[*m*-(TPP-DEHMP)]M (M = H_2, Zn), where *p*-(TPP-DEHMP) is the tetraanion of 1-[5-(10,15,20-triphenylporphyrinyl)]-4-[10-(2,18-diethyl-3,7,8,12,13,17- hexamethylporphyrinyl)]benzene and *m*-(TPP-DEHMP) is the tetraanion of 1-[5-(10,15,20-triphenylporphyrinyl)]-3-[10-(2,18-diethyl-3,7,8,12,13,17-hexamethylporphyrinyl)]benzene. The photophysical properties of the heteroleptic dimers are compared to those of monomeric (TPP)H_2, [(10-Ph)DEHMP]H_2, (TPP)Zn, and [(10-Ph)DEHMP]-Zn as well as those of dimeric M[*p*-(TPP-TPP)]M and M[*m*-(TPP-TPP)]M (M = H_2, Zn), where TPP is the dianion of tetraphenylporphyrin, (10-Ph)DEHMP is the dianion of 10-phenyl-(2,18-diethyl-3,7,8,12,13,17-hexamethyl)porphyrin, *p*-(TPP-TPP) is the tetraanion of 1,4-bis[5′-(10′,15′,20′-triphenylporphyrinyl)]benzene, and *m*-(TPP-TPP) is the tetraanion of 1,3-bis[5′-(10′,15′,20′-triphenylporphyrinyl)]benzene. The electrochemical and spectroelectrochemical properties of Zn[*p*-(TPP-DEHMP)]Zn were also examined in order to ascertain whether any electronic interactions exist in the neutral, reduced, or oxidized forms of the investigated compounds. Structures of the heteroleptic and homoleptic dimers are shown in Figure 1 which also includes a schematic representation of the related monomeric units.

Results and Discussion

Electronic Absorption Spectra. The spectrum of Zn[*p*-(TPP-DEHMP)]Zn in PhCN containing 0.2 M TBAP is characterized by two Soret bands at 414 and 431 nm, two visible bands centered at 550 and 598 nm, and a shoulder at about 575

(5) Wasielewski, M. R. In *Photoinduced Electron Transfer*, *Part A*; Fox, M. A., Chanon, M., Eds.; Elsevier: Amsterdam, 1988; p 161.

(6) (a) Bensasson, R. V.; Land, E. J.; Moore, A. L.; Crouch, R. L.; Dirks, G.; Moore, T. A.; Gust, D. *Nature* **1981**, *290*, 329. (b) Moore, A. L.; Joy, A.; Tom, R.; Gust, D.; Moore, T. A.; Bensasson, R. V.; Land, E. J. *Science* **1982**, *216*, 982. (c) Selensky, R.; Holten, D.; Windsor, M. W.; Paine, J. B., III; Dolphin, D.; Gouterman, M.; Thomas, J. C. *Chem. Phys.* **1981**, *60*, 33. (d) Wasielewski, M. R.; Niemczyk, M. P.; Svec, W. A. *Tetrahedron Lett.* **1982**, *23*, 3215. (e) Mialocq, J. C.; Giannotti, C.; Maillard, P.; Momentau, M. *Chem. Phys. Lett.* **1984**, *112*, 87. (f) Regev, A.; Galili, T.; Levanon, H.; Harriman, H. *Chem. Phys. Lett.* **1986**, *131*, 140. (g) Gonen, O.; Levanon, H. *Chem. Phys.* **1986**, *84*, 4132. (h) Brookfield, R. L.; Ellul, H.; Harriman, A.; Porter, G. *J. Chem. Soc., Faraday Trans. 2* **1986**, *82*, 219. (i) Davila, J.; Harriman, A.; Milgrom, L. R. *Chem. Phys. Lett.* **1987**, *136*, 427. (j) Noblat, S.; Dietrich-Buchecker, C. O.; Sauvage, J. P. *Tetrahedron Lett.* **1987**, *28*, 5829. (k) Chardon-Noblat, S.; Sauvage, J. P.; Mathis, P. *Angew. Chem., Int. Ed. Engl.* **1989**, *28*, 593. (l) Rempel, U.; Von Maltzan, B.; Von Borczyskowski, C. *Chem. Phys. Lett.* **1990**, *169*, 347. (m) Osuka, A.; Maruyama, K.; Yamazaki, I.; Tamai, N. *Chem. Phys. Lett.* **1990**, *165*, 392. (n) Sessler, J. L.; Johnson, M. R.; Creager, S. F.; Fettinger, J. C.; Ibers, J. A. *J. Am. Chem. Soc.* **1990**, *112*, 9310. (o) Wasielewski, M. R.; Johnson, D. G.; Niemczyk, M. P.; Gaines, G. L.; O'Neil, M. P.; Svec, V. A. *J. Am. Chem. Soc.* **1990**, *112*, 6482. (p) Gust, D.; Moore, T. A.; Moore, A. L.; Gao, F.; Luttrull, D.; De Graziano, J. M.; Ma, X. C.; Makings, L. R.; Lee, S. J.; Trier, T. T.; Bittersmann, E.; Seely, G. R.; Woodward, S.; Bensasson, R. V.; Rougée, M.; De Schryver, F. C.; Van der Auweraer, M. *J. Am. Chem. Soc.* **1991**, *113*, 3638. (q) Helms, A.; Heiler, D.; McLendon, G. *J. Am. Chem. Soc.* **1992**, *114*, 6227. (r) Gust, D.; Moore, T. A.; Moore, A. L.; Leggett, L.; Lin, S.; De Graziano, J. M.; Hermant, R. M.; Nicodem, D.; Craig, P.; Seely, G. R.; Nieman, R. A. *J. Phys. Chem.* **1993**, *97*, 7926. (s) Osuka, A.; Nakajima, S.; Maruyama, K.; Mataga, N.; Asahi, T.; Yamazaki, I.; Nishimura, Y.; Ohno, T.; Nozaki, K. *J. Am. Chem. Soc.* **1993**, *115*, 4577. (t) Sessler, J. L.; Capuano, V. L.; Harriman, H. *J. Am. Chem. Soc.* **1993**, *115*, 4618. (u) Gust, D.; Moore, T. A.; Moore, A. L.; Krasnovsky, A. A. Jr.; Liddell, P. A.; Nicodem, D.; De Graziano, J. M.; Kerrigan, P.; Makings, L. R.; Pessiki, P. J. *J. Am. Chem. Soc.* **1993**, *115*, 5684. (v) De Graziano, J. M.; Liddel, P. A.; Leggett, L.; Moore, A. L.; Moore, T. A.; Gust, D. *J. Phys. Chem.* **1994**, *98*, 1758. (w) Harriman, A.; Heitz, V.; Ebersole, M.; Van Willigen, H. *J. Phys. Chem.* **1994**, *98*, 4892. (x) Osuka, A.; Tanabe, N.; Kawabata, S.; Yamazaki, I.; Nishimura, Y. *J. Org. Chem.* **1995**, *60*, 7177. (y) Osuka, A.; Nakajima, S.; Okada, T.; Taniguchi, S.; Nozaki, K.; Ohno, T.; Yamazaki, I.; Nishimura, Y.; Mataga, N. *Angew. Chem., Int. Ed. Engl.* **1996**, *35*, 92. (z) Wagner, R. W.; Johnson, T. E.; Lindsey, J. S. *J. Am. Chem. Soc.* **1996**, *118*, 11166.

(7) (a) Hunter, C. A.; Sarson, L. D. *Angew. Chem., Int. Ed. Engl.* **1994**, *33*, 2313. (b) Sessler, J. L.; Wang, B.; Harriman, A. *J. Am. Chem. Soc.* **1995**, *117*, 704. (c) Král, V.; Springs, S. L.; Sessler, J. L. *J. Am. Chem. Soc.* **1995**, *117*, 8881.

(8) (a) Paolesse, R.; Pandey, R. K.; Forsyth, T. P.; Jaquinod, L.; Gerzevske, K. R.; Senge, M. O.; Licoccia, S.; Boschi, T.; Smith, K. M. *J. Am. Chem. Soc.* **1996**, *118*, 3869. (b) Paolesse, R.; Tagliatesta, P.; Boschi, T. *Tetrahedron Lett.* **1996,** *37*, 2637.

(9) Setsune, J.; Yoshida, H.; Ogoshi, H. *J. Chem. Soc., Perk. Trans. 1* **1982**, 983.

I. Monomers

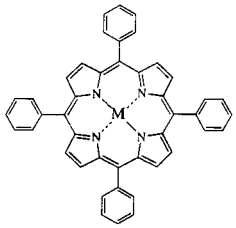

(TPP)M

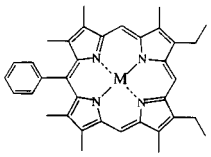

[(10-Ph)DEHMP]M

II. Heterodimers

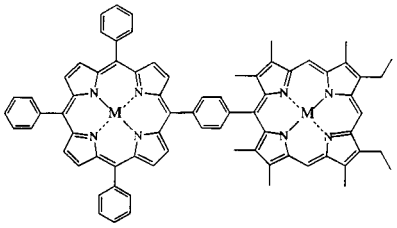

M[*p*-(TPP-DEHMP)]M

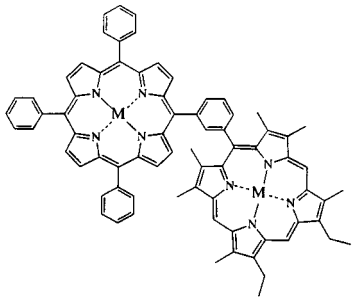

M[*m*-(TPP-DEHMP)]M

III. Homodimers

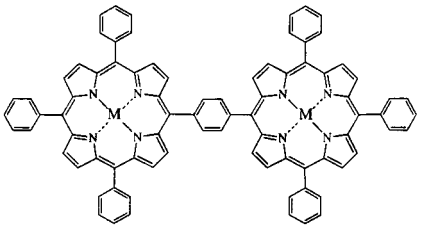

M[*p*-(TPP-TPP)]M

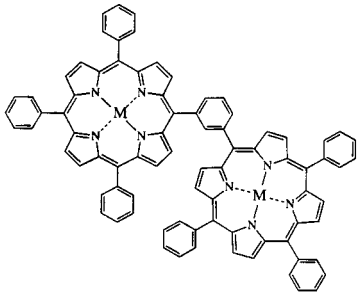

M[*m*-(TPP-TPP)]M

Figure 1. Schematic representation of investigated compounds.

Table 1. UV−Visible Spectral Data of H_2[*p*-TPP-DEHMP)]H_2, Zn[*p*-(TPP-DEHMP)]Zn, and Their Related Monomeric Subunits, (TPP)M and (OEP)M, Where M = H_2 or Zn

	λ_{max}, nm	
compound	Soret band	visible bands
Zn[*p*-(TPP-DEHMP)]Zn	414, 431	550,[a] 575 (sh), 598
(TPP)Zn	427	556, 600
(OEP)Zn	410	536, 572
H_2[*p*-TPP-DEHMP)]H_2	411 (sh), 425	511, 549, 571, 591, 625, 650
(TPP)H_2	432	516, 551, 591, 648
(OEP)H_2	408	571, 625

[a] Broad band which results from the overlap of bands at 536 and 556 nm; sh, shoulder.

nm. Under the same experimental conditions, the spectrum of (OEP)Zn has bands at 410, 536, and 572 nm while the spectrum of (TPP)Zn has bands at 427, 556, and 600 nm (see Table 1). The UV−visible spectrum of Zn[*p*-(TPP-DEHMP)]Zn thus closely resembles that of superposed (TPP)Zn and (OEP)Zn. The absorption bands of Zn[*p*-(TPP-DEHMP)]Zn at 414 and 575 nm are similar to the absorption bands of (OEP)Zn at 410 and 572 nm and can thus be assigned to the (DEHMP)Zn part of the dimer. At the same time, the bands of the dimer at 431, 550, and 598 nm correspond to the spectral features of (TPP)-Zn at 427, 556, and 600 nm and can thus be assigned to the TPP part of the dimer. The spectral features of (TPP)H_2, (OEP)-H_2, and H_2[*p*-(TPP-DEHMP)]H_2 are also listed in Table 1 and show that the UV−visible spectrum of H_2[*p*-(TPP-DEHMP)]-H_2 is also similar to superposed UV−visible spectra of monomeric (TPP)H_2 and (OEP)H_2.

Small differences exist between the peak maxima of the dimer and those of its two monomeric components for both Zn[*p*-(TPP-DEHMP)]Zn and H_2[*p*-(TPP-DEHMP)]H_2. These might be accounted for by the addition of two overlapping spectra which results in an apparent shift of the maxima, a small interaction between the two macrocycles, or alternatively by the fact that the monomeric TPP and OEP macrocycles used for comparison purposes are not identical structural units in the combined TPP-DEHMP macrocycle (see Figure 1). However, the close similarity between the UV−visible spectrum of M[*p*-(TPP-DEHMP)]M (M = Zn, H_2) and that of combined (OEP)M and (TPP)M (M = Zn, H_2) implies that there is little or no

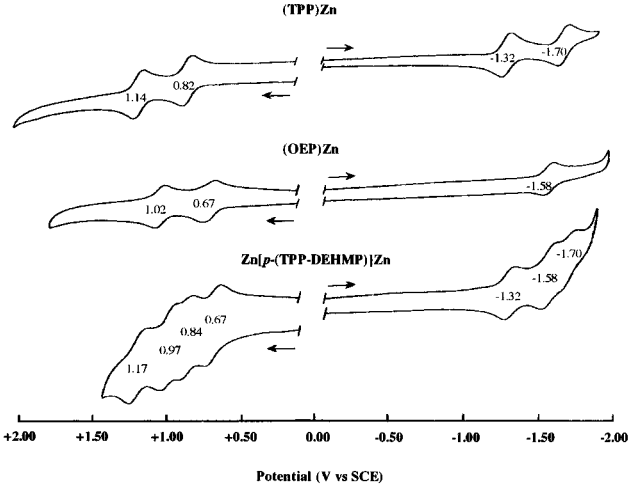

Figure 2. Cyclic voltammograms of Zn[*p*-(TPP-DEHMP)]Zn, (OEP)-Zn, and (TPP)Zn in PhCN containing 0.1 M TBAP.

conjugation between the TPP and DEHMP subunits in the neutral dimeric array. The electrochemistry of Zn[*p*-(TPP-DEHMP)]Zn, which is discussed below, also leads to the same conclusion.

Electrochemistry and UV−Visible Spectroelectrochemistry of Zn[*p*-(TPP-DEHMP)]Zn. Figure 2 illustrates the room-temperature cyclic voltammograms of (TPP)Zn, (OEP)Zn, and Zn[*p*-(TPP-DEHMP)]Zn in PhCN, 0.1 M TBAP. Zn[*p*-(TPP-DEHMP)]Zn undergoes three reversible one-electron reductions and four one-electron oxidations between +1.50 and −2.00 V. The reductions of the dimer occur at $E_{1/2} = -1.32$, −1.58, and −1.70 V. The $E_{1/2}$ values for the first and third processes are identical to $E_{1/2}$ values for the first and second reductions of (TPP)Zn, while $E_{1/2}$ for the second reduction of Zn[*p*-(TPP-DEHMP)]Zn is identical to that for the first reduction of (OEP)-Zn (see Figure 2). These data suggest that the first and third reductions of Zn[*p*-(TPP-DEHMP)]Zn involve the (TPP)Zn part of the dimer while the second reduction involves the (−DEHMP)Zn subunit. The oxidation of Zn[*p*-(TPP-DEHMP)]Zn also occurs via stepwise electrode processes involving alternately the TPP and DEHMP parts of the dimer. As shown in Figure 2, the $E_{1/2}$ values for the first and third oxidations of the compound ($E_{1/2} = 0.67$ and 0.97 V) are similar to $E_{1/2}$ for the first and second oxidations of (OEP)Zn ($E_{1/2} = 0.67$ and 1.02 V) while the second and fourth oxidations of Zn[*p*-(TPP-DEHMP)]Zn ($E_{1/2} = 0.84$ and 1.17 V) occur at virtually identical potentials as the first and second oxidations of (TPP)-Zn ($E_{1/2} = 0.82$ and 1.14 V). The site of electron transfer upon the first reduction and first oxidation of Zn[*p*-(TPP-DEHMP)]-Zn was confirmed by measurement of the UV−visible absorption spectra of the singly reduced and singly oxidized dimers as discussed below.

The UV−visible spectra of neutral, singly oxidized, and singly reduced Zn[*p*-(TPP-DEHMP)]Zn are shown in Figure 3. As discussed earlier, the spectral features of the neutral compound (Figure 3a) can be approximated by a simple superposition of the electronic absorption spectra of (TPP)Zn and (OEP)Zn. The UV−visible spectrum obtained upon abstraction of a single electron from the dimer has a single well-defined Soret band at 431 nm and three visible bands at 557, 598, and 660 nm (see Figure 3b). The loss of the 414 nm band and the presence of a new band at 660 nm are consistent with the abstraction of one-electron from the (−DEHMP)Zn subunit and a subsequent formation of the porphyrin π cation radical,

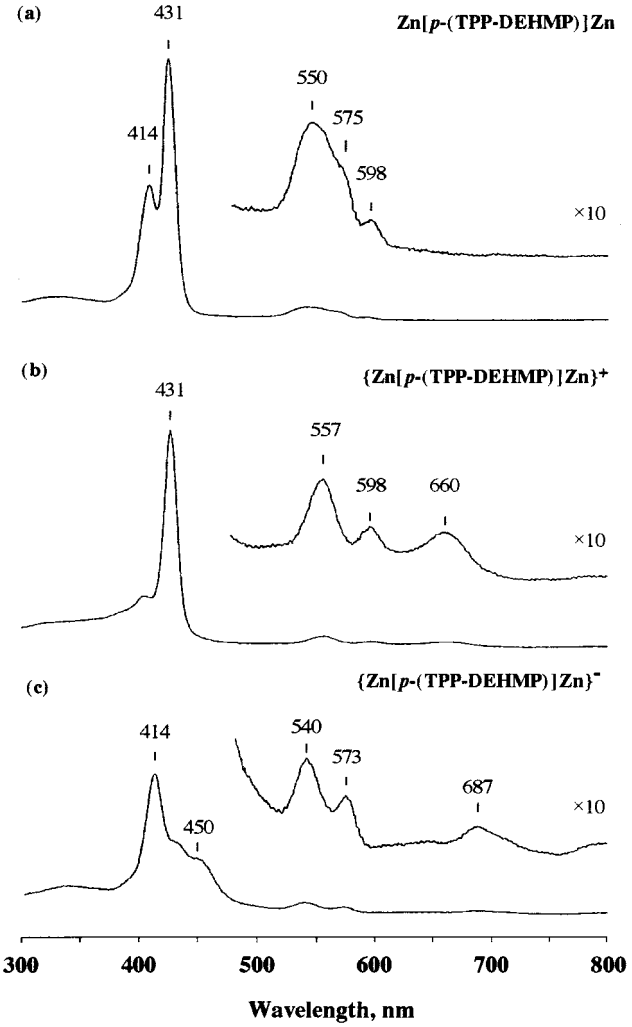

Figure 3. Thin-layer electronic absorption spectra of (a) neutral, (b) singly oxidized, and (c) singly reduced Zn[*p*-(TPP-DEHMP)]Zn in PhCN, 0.2 M TBAP.

{Zn[*p*-(TPP-DEHMP•)]Zn}$^+$. Indeed, the electrogeneration of [(OEP•)Zn]$^+$ from (OEP)Zn, under the same experimental conditions, leads to similar spectral features.[10]

The UV−visible spectrum obtained upon addition of one electron to Zn[*p*-(TPP-DEHMP)]Zn is shown in Figure 3c. This spectrum differs from that of neutral Zn[*p*-(TPP-DEHMP)]Zn in that it shows a well-defined 414 nm band (which was assigned to the DEHMP part of the molecule) and a loss of the 431 nm band (which was assigned to the TPP part of the molecule). There are also well-defined new absorption bands located at 450, 540, 573, and 687 nm. The electronic absorption spectrum of the porphyrin π anion radical, [(TPP•)Zn]$^-$, is characterized by bands at 454 and 705 nm[11] while neutral (OEP)Zn has two visible bands at 536 and 572 nm (see Table 1). Hence, the spectral data in Figure 3c imply that the first reduction of Zn-[*p*-(TPP-DEHMP)]Zn involves the (TPP)Zn subunit and leads to the tetraphenyl porphyrin π anion radical, {Zn[*p*-(TPP•-DEHMP)]Zn}$^-$.

Photochemistry. Fluorescence and phosphorescence spectra, as well as singlet and triplet lifetimes of the symmetrical

(10) Oxidation of (OEP)Zn at 0.80 V in PhCN, 0.2 M TBAP, is accompanied by a large decrease of the Soret band and a concomitant increase of a new absorption band at 655 nm.

(11) Felton, R. H. in *The Porphyrins*; Dolphin, D., Ed.; Academic Press: New York, 1978; Vol. 5, p 72.

Table 2. Luminescence Properties[a] in 2-Methyltetrahydrofurane

	fluorescence					phosphorescence	
	room temperature			77 K		77 K	
compound	λ_{max}	τ	Φ	λ_{max}	τ	λ_{max}	τ
[(10-Ph)DEHMP]H_2	629	15.8	0.13	621	26.0		
(TPP)H_2	652	13.1	0.10	643	14.8		
H_2[*p*-(TPP-TPP)]H_2	654	11.8	0.12	649	13.7		
H_2[*m*-(TPP-TPP)]H_2	651	12.6	0.11	645	14.7		
H_2[*p*-(TPP-DEHMP)]H_2	624	13.2		618	15.8		
	654	3.3		645	3.3		
H_2[*m*-(TPP-DEHMP)]H_2	624	13.1		619	13.8		
	654	1.1		646	1.2		
[(10-Ph)DEHMP]Zn	581	1.9	0.034	576	2.2	706	81.4
(TPP)Zn	602	2.1	0.031				
Zn[*p*-(TPP-TPP)]Zn	602	2.0	0.033	607	2.5	790	19.4
Zn[*m*-(TPP-TPPP)]Zn	606	2.1	0.029	604	2.8	789	17.5
Zn[*m*-(TPP-DEHMP)]Zn	602	2.0	0.029	602		787	16.4

[a] λ_{max} in nm; τ in ns.

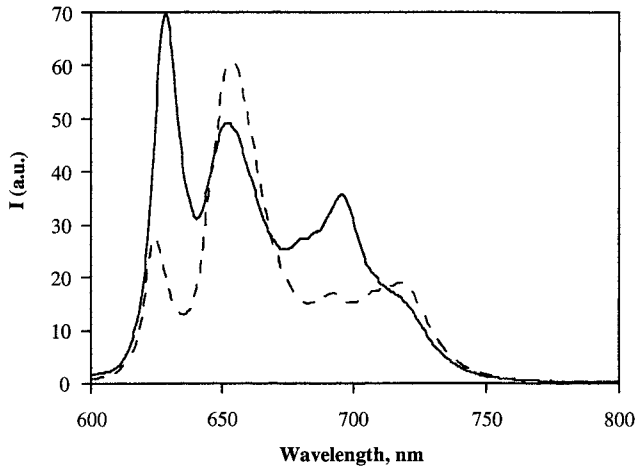

Figure 4. Emission spectrum of H_2[*m*-(TPP-DEHMP)]H_2 (- - -) and an equimolar solution of [(10-Ph)DEHMP]H_2 and (TPP)H_2 (—) at room temperature in 2-methyltetrahydrofurane (λ_{exc} = 500 nm).

porphyrin dimers, H_2[*p*-(TPP-TPP)]H_2 and H_2[*m*-(TPP-TPP)]-H_2, are only slightly modified with respect to those of their monomeric (TPP)H_2 units (see Table 2), and this result shows that the interaction between the two TPP subunits is, in all cases, relatively weak. Furthermore, the only additional pathway responsible for a radiationless decay to the ground state occurs via an electron transfer between the two porphyrin units of H_2-[*p*-(TPP-TPP)]H_2 or H_2[*m*-(TPP-TPP)]H_2, a process which is thermodynamically forbidden in the case of such dimers.

The luminescence spectra of the asymmetric porphyrin dimers are not simply obtained by adding the spectra of their two monomeric porphyrins. As shown in Figure 4 and Table 2, the fluorescence intensities and lifetimes of the DEHMP components in H_2[*p*-(TPP-DEHMP)]H_2 and H_2[*m*-(TPP-DEHMP)]H_2 are considerably quenched, both at room temperature and 77 K. The luminescence intensities of the DEHMP component is decreased by a factor of 4.8 for H_2[*p*-(TPP-DEHMP)]H_2 and 14 for H_2[*m*-(TPP-DEHMP)]H_2 at room temperature. In contrast, the emission intensity of the TPP unit in both dimers is higher than that obtained by adding the emission intensities of the two individual monomeric (TPP)H_2 subunits.

The excitation spectra of the heterodimers provide information about their photochemical behavior. When the monochromator is set to conditions where 100% of the total luminescence is due to the DEHMP component, i.e., at λ_{em} = 628 nm, the excitation spectrum resembles the absorption spectrum of the

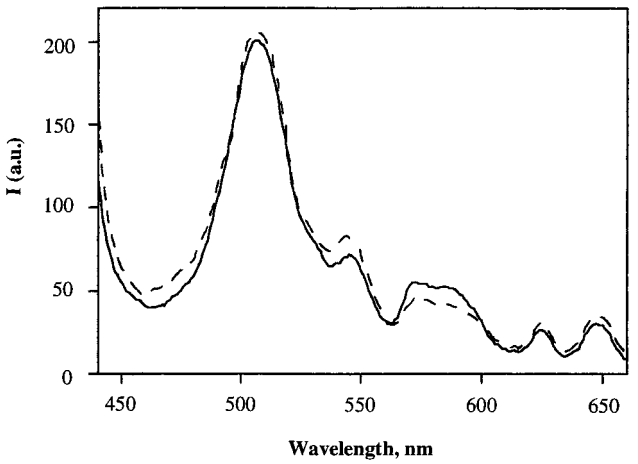

Figure 5. Absorption spectrum (—) and excitation spectrum (- - -) (λ_{em} = 725 nm) of H_2[*m*-(TPP-DEHMP)]H_2 in 2-methyltetrahydrofurane.

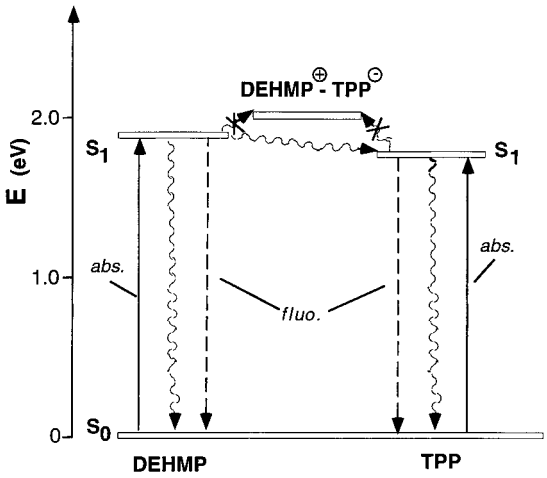

Figure 6. Energy level diagram of H_2[*p*-(TPP-DEHMP)]H_2 and H_2-[*m*-(TPP-DEHMP)]H_2 (only one diagram is shown) at room temperature. The energy of charge transfer state ($DEHMP^+$-TPP^-) is calculated by using the $E_{1/2}$ for reduction of (TPP)H_2 and $E_{1/2}$ for oxidation of (OEP)H_2 in CH_2Cl_2.

DEHMP moiety alone. However, under conditions where the fluorescence is almost entirely (>95%) due to the TPP component, i.e., at λ_{em} = 725 nm, the excitation spectrum of H_2[*m*-(TPP-DEHMP)]H_2 is very similar (Figure 5) to the absorption spectrum of the same compound in that it shows bands for both the TPP and DEHMP components. These data therefore indicate that an efficient energy transfer occurs between the DEHMP and the TPP moieties of H_2[*p*-(TPP-DEHMP)]H_2 and H_2[*m*-(TPP-DEHMP)]H_2.

Figure 6 shows an energy-level diagram of H_2[*p*-(TPP-DEHMP)]H_2 and H_2[*m*-(TPP-DEHMP)]H_2 which indicates the processes likely to take place after excitation of one of the two moieties. A transfer of energy from DEHMP to TPP is thermodynamically allowed, whereas an electron transfer is, at least in nonpolar solvents as 2-methyltetrahydrofurane, slighthly endoergonic.

The rate constant of the quenching process does not vary upon a decrease of temperature (vide infra), and this suggests that the energy transfer process is by far the preferred deactivation mechanism. Indeed, a deactivation mechanism involving electron transfer, rather than energy transfer, between the two porphyrin moieties would have resulted in a smaller value of the rate constant upon a lowering of the temperature. The rate constants of energy transfer were calculated using eq 1, where

τ_0 is the unquenched lifetime of the parent compound and τ is the quenched lifetime of the DEHMP moiety in the asymmetric diporphyrin systems.

$$k_e = \frac{1}{\tau} - \frac{1}{\tau_0} \quad (1)$$

The rate constant, k_e, was calculated at room temperature and was found to be 2.4×10^8 s^{-1} for H_2[*p*-(TPP-DEHMP)]H_2 and 8.5×10^8 s^{-1} for H_2[*m*-(TPP-DEHMP)]H_2. The efficiency of energy transfer from the DEHMP to the TPP moiety in each heterodimer was determined by using their respective calculated values of k_e and was found to be 0.79 for H_2[*p*-(TPP-DEHMP)]-H_2 and 0.93 for H_2[*m*-(TPP-DEHMP)]H_2. Similar calculations were also performed at 77 K, and k_e values of 2.6×10^8 and 7.9×10^8 s^{-1} were determined for H_2[*p*-(TPP-DEHMP)]H_2 and H_2[*m*-(TPP-DEHMP)]H_2, respectively. The overall data show that the quenching process depends neither on the temperature nor on the rigidity of the solvent.

The energy transfer process between the DEHMP and TPP macrocycles of Zn[*m*-(TPP-DEHMP)]Zn is even faster than that between the DEHMP and TPP subunits of Zn[*p*-(TPP-DEHMP)]-Zn and a fluorescence due to the (−DEHMP)Zn moiety is no longer observed, either at room temperature or at 77 K. In this case, the efficiency of the process is >0.99, and a limiting value of 2.5×10^{10} s^{-1} can be calculated for the rate constant of the quenching process.

It is noteworthy to compare the experimentally determined rate constants with theoretically calculated values. These energy transfer processes can be described in terms of Coulombic (Föster)[12] or exchange (Dexter)[13] mechanisms, the former of which was used to explain the experimental data obtained with similar diporphyrin systems.[6m,t] In the Föster mechanism, the energy transfer rate constant can be estimated by calculating J_F (eq 2), which stands for the overlap integral between the emission spectrum of the donor $F(\nu)$ (normalized by the equation $\int F(\nu)\delta\nu = 1$) and the absorption spectrum of the acceptor ϵ-(ν).

$$J_F = \frac{\int F(\nu)\epsilon(\nu)\nu^{-4}\mathrm{d}\nu}{\int F(\nu)\mathrm{d}\nu} \quad (2)$$

The overlap integrals, J_F, were found to be 1.3×10^{-15} cm^{-3} M^{-1} for both H_2[*p*-(TPP-DEHMP)]H_2 and H_2[*m*-(TPP-DEHMP)]H_2 (in which the donor and acceptor moieties are identical in the two systems) but 3.2×10^{-14} cm^{-3} M^{-1} for Zn[*m*-(TPP-DEHMP)]Zn.

The energy transfer rate constant is given by eq 3

$$k_e = \frac{8.8 \times 10^{-25} K^2 \Phi}{n^4 \tau r^6} J_F \quad (3)$$

where n is the refraction index of the solvent, Φ the luminescence quantum yield, τ the lifetime of the donor, r the distance between the donor and acceptor molecules, J_F the overlap integral, and K^2 a geometric factor. The value of the latter parameter depends on the relative orientation of the dipoles and in our case can be taken with good confidence as $^2/_3$.[12] If one assumes that the distance from center to center is 12.8 Å for H_2[*p*-(TPP-DEHMP)]H_2 and 10.5 Å for both H_2[*m*-(TPP-DEHMP)]H_2 and Zn[*m*-(TPP-DEHMP)]Zn,[7b] the calculated rate constants would be 3.6×10^8 s^{-1} for H_2[*p*-(TPP-DEHMP)]H_2, 1.3×10^9 s^{-1} for H_2[*m*-(TPP-DEHMP)]H_2, and 6.0×10^{10} s^{-1} for Zn[*m*-(TPP-DEHMP)]Zn. These values agree well with the experimental results.

Recently, Lindsey and co-workers reported a detailed study of energy transfer processes occurring in ethyne-linked TPP dimers and trimers.[14] These compounds differ from the TPP-DEHMP dimers in that the energy transfer from a Zn porphyrin to a free base porphyrin is demonstrated to occur primarily via a Dexter mechanism. This different behavior is probably due to the nature of the bridging group. In TPP-DEHMP dimers the macrocycles cannot be coplanar with the bridging phenyl group owing to steric repulsions, thus excluding direct conjugation between the π systems of porphyrins and the linker. This hypothesis is consistent with the Lindsey's report that coplanarity is important for an efficient through bond energy transfer process.[14] In fact, the introduction of steric constraints in the ethyne-linked dimers enhance the participation of the through space mechanism in the overall energy transfer process.

Finally, it should be pointed out that for each asymmetric diporphyrin system investigated here, the back energy transfer from the singlet excited state of TPP to that of the DEHMP moiety does not compete with a deactivation to the ground state. This is explained by the fact that the emission spectrum of TPP and the absorption spectrum of DEHMP poorly overlap (eqs 2 and 3). Consequently, the energy transfer between DEHMP and TPP can be envisioned as a unidirectional process.

Conclusion

Detailed photophysical and electrochemical studies of free base and zinc-metalated *p*-(TPP-DEHMP) and *m*-(TPP-DEHMP) dimers clearly show that electronic interactions between the two subunits are very weak. In fact, the absorption spectra and the electrochemical properties of the dimers can be described by a superposition of the two monomeric subunits.

Very interestingly, however, both the free base and Zn derivatives of *p*-(TPP-DEHMP) and *m*-(TPP-DEHMP) undergo an efficient energy transfer process between the DEHMP and the TPP moieties. Emission and excitation spectra recorded at room temperature and 77 K show that a deactivation mechanism via energy transfer is by far predominant with respect to a deactivation mechanism involving an electron transfer as suggested by thermodynamical considerations. The experimental energy transfer rate constants also agree with the values predicted by the Föster theory.

The individual character of each macrocycle is conserved in these dimers; their novelty with respect to previously reported porphyrin arrays lies in the fact that energy transfer is not incoherent but that the DEHMP moiety of each dimer acts as an antenna for the corresponding TPP subunit.

Experimental Section

Instrumentation. Electronic UV−visible absorption spectra were recorded on a Perkin-Elmer λ16 spectrophotometer or on a Philips PU8700 spectrophotometer. Uncorrected emission, corrected excitation spectra, and phosphorescence lifetimes were obtained with a Perkin-Elmer LS50 spectrofluorometer.

The fluorescence lifetimes (uncertainty, ±5%) were obtained with an Edinburgh single-photon counting apparatus, in which the flash lamp was filled with N_2. Emission spectra at 77 K in a 2-methyltetrahy-

(12) Föster, T. *Discuss. Faraday Soc*. **1959**, *27*, 7.
(13) Dexter, D. L. *J. Chem. Phys.* **1953**, *21*, 836.
(14) (a) Hsiao, J.-S.; Krueger, B. P.; Wagner, R. W.; Johnson, T. E.; Delaney, J. K.; Mauzerall, D. C.; Fleming, G. R.; Lindsey, J. S.; Bocian, D. F.; Donohoe, R. J *J. Am. Chem. Soc*. **1996**, *118*, 11181. (b) Seth, J.; Palaniappan, V.; Wagner, R. W.; Johnson, T. E.; Lindsey, J. S.; Bocial, D. F. *J. Am. Chem. Soc*. **1996**, *118*, 11194.

drofurane rigid transparent matrix were recorded using quartz tubes immersed in a quartz Dewar filled with liquid nitrogen. Fluorescence quantum yields were determined using $(TPP)H_2$ ($\Phi = 0.11$) or (TPP)-Zn ($\Phi = 0.030$) in deaerated toluene.[15] $Ru(bpy)_3^{2+}$ ($\Phi = 0.028$ in aerated water solution)[16] was used as an additional standard. To allow a comparison of emission intensities, corrections for different absorbance[17] and phototube sensitivity were performed. A correction for a difference in the refraction index was introduced when necessary. The solutions were degassed with a freeze−thaw−pump method. ^{1}H NMR spectra were recorded on a Bruker AM 400 spectrometer as $CDCl_3$ solutions. Chemical shifts are given in ppm from tetramethylsilane (TMS) and are referenced against residual solvent signals. Mass spectra (FAB) were recorded on a VG-Quattro spectrometer using nitrobenzyl alcohol (NBA) as a matrix.

Cyclic voltammetry was carried out on an EG&G model 173 potentiostat or an IBM model EC 225 Voltammetric Analyzer. Current−voltage curves were recorded on an EG&G Princeton Applied Research model RE-0151 X-Y recorder. A three-electrode system was used and consisted of a platinum button working electrode, a platinum wire counter electrode, and a saturated calomel reference electrode (SCE). The reference electrode was separated from the bulk of the solution by a fritted-glass bridge filled with the solvent/supporting electrolyte mixture. High-purity-grade N_2 was used to deoxygenate the solution before each experiment. All potentials are reported versus the SCE.

UV−visible spectroelectrochemical experiments were performed with an optically transparent thin-layer spectroelectrochemical cell described in the literature.[18] Potentials for oxidation or reduction of each complex were applied with an EG&G model 173 potentiostat. Time-resolved spectra were recorded with a Hewlett-Packard model 8453 diode array spectrophotometer.

Elemental analyses were carried out by the Microanalytical Laboratory at the University of Padova, Italy.

Chemicals. Silica gel 60 (70−230 and 230−400 mesh, Merck) or neutral alumina (Merck; usually Brockmann Grade III, i.e., deactivated with 6% water) was used for column chromatography. Benzonitrile (PhCN) was purchased from Aldrich Chemical Co. and distilled over P_2O_5 under vacuum prior to use. Absolute dichloromethane (CH_2Cl_2) over molecular sieves was obtained from Fluka Chemical Co. and used without further purification. Tetra-*n*-butylammonium perchlorate (TBAP) and tetra-*n*-butylammonium hexafluorophosphate ($TBAPF_6$), from Fluka Chemical Co., were recrystallized from ethyl alcohol and ethyl acetate, respectively, and dried under vacuum at 40 °C for at least 1 week prior to use. High-purity-grade nitrogen gas was purchased from Trigas (Houston). All other reagents and solvents were from Fluka, Aldrich, or Carlo Erba and were used as received.

Synthesis. The syntheses of 1-[5-(10,15,20-triphenylporphyrinyl)]-4-[10-(2,18-diethyl-3,7,8,12,13,17-hexamethylporphyrinyl)]benzene, H_2-[*p*-(TPP-DEHMP)]H_2, and 1-[5-(10,15,20-triphenylporphyrinyl)]-3-[10-(2,18-diethyl-3,7,8,12,13,17-hexamethylporphyrinyl)]benzene, H_2[*m*-(TPP-DEHMP)]H_2, which are reported here follow the reaction pathway illustrated in Scheme 1.[19]

The alkyl porphyrin part of such dimers can reasonably be considered very similar to octaethylporphyrin (OEP), and on the basis of their similar structure, one can assume that OEP and DEHMP macrocycles should have similar electrochemical and spectral properties.

Metal complexes of H_2[*p*-(TPP-DEHMP)]H_2 and H_2[*m*-(TPP-DEHMP)]H_2 (see Figure 1) were prepared according to usual metalation procedures.[20] The first porphyrin to be metalated is the DEHMP macrocycle in all cases, and this is explained by the better donor properties of such porphyrin moiety. This difference in reactivity toward metalation has been used to synthesize monometalated porphyrin dimers.[20] Symmetrical H_2[*p*-(TPP-TPP)]H_2 and H_2[*m*-(TPP-TPP]H_2

Scheme 1

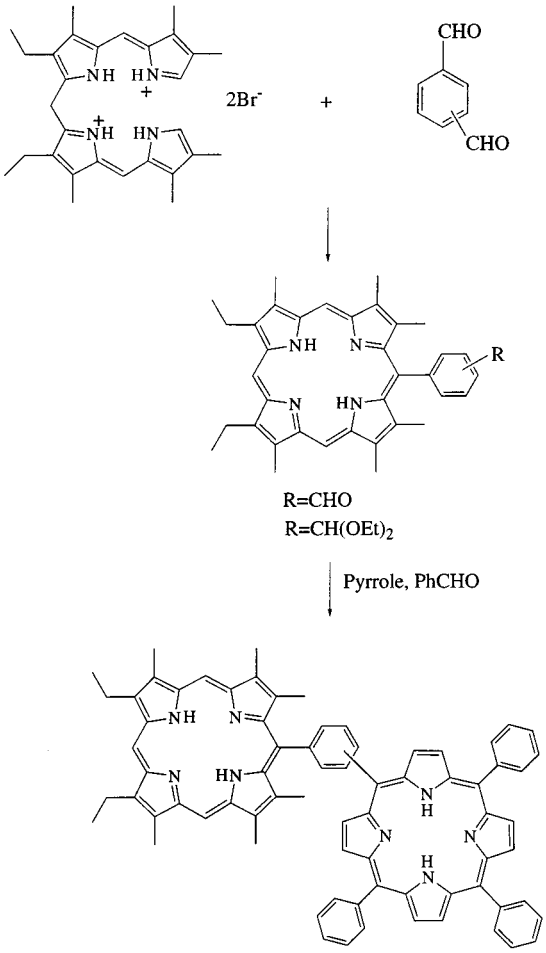

dimers and their zinc complexes were also prepared following methods previously reported in the literature.[21]

10-(4′-Formylphenyl)-(2,18-diethyl-3,7,8,12,13,17-hexamethyl)-porphyrin, [(10-Ph-4′-CHO)DEHMP]H_2. (8,12-Diethyl-2,3,7,13,17,18-hexamethyl)-*a*,*c*-biladiene salt (500 mg), terephthaldehyde (500 mg), and 4-toluenesulfonic acid (TsOH) (1 g) were dissolved in ethanol and refluxed for 4 h. Sodium acetate was added to neutralize the solution, and the solvent was evaporated under vacuum. The residue was dissolved in CH_2Cl_2 and chromatographed on silica gel using CH_2Cl_2 as eluent. A first red-violet band afforded the title product. After elution with a CH_2Cl_2/methanol (98/2) mixture, a second red-brown band was collected and gave the diethyl acetal of [(10-Ph-4′-CHO)-DEHMP]H_2. The corresponding porphyrin aldehyde was obtained by washing a CH_2Cl_2 solution of the acetal with 2 N HCl and then with saturated $NaHCO_3$. A subsequent crystallization from a CH_2Cl_2/methanol mixture afforded quantitatively [(10-Ph-4′-CHO)DEHMP]-H_2 as red-violet microcrystals (309 mg, 67%). UV−vis: λ_{max} nm, 404, 503, 536, 570, 624. ^{1}H NMR (δ ppm, $CDCl_3$): 10.38 (s, 1H), 10.11 (s, 2H), 9.92 (s, 1H), 8.22 (s, 4H), 4.16 (q, 4H), 3.52 (s, 12H), 2.41 (s, 6H), 1.92 (t, 6H), −3.18 (br s, 2H). FAB-MS: 555 $[M]^+$. Anal. Calcd for $C_{37}H_{38}N_4O$: C, 80.11; H, 6.90; N, 10.10. Found: C, 80.12; H, 6.91; N, 10.04.

10-(3′-Formylphenyl)-8,12-diethyl-2,3,7,13,17,18-hexamethylporphyrin, [(10-Ph-3′-CHO)DEHMP]H_2. This porphyrin (295 mg, 64% yield) was prepared as above from (8,12-diethyl-2,3,7,13,17,18-hexamethyl)-*a*,*c*-biladiene and isophthalaldehyde. UV−vis: λ_{max} nm, 403, 504, 536, 570, 623. ^{1}H NMR (δ ppm, $CDCl_3$): 10.35 (s, 1H), 10.15 (s, 2H), 9.89 (s, 1H), 7.82−7.52 (m, 4H), 4.12 (q, 4H), 3.48 (s, 12H), 2.52 (s, 6H), 1.99 (t, 6H), −3.21 (br s, 2H). FAB-MS: 555

(15) Seybold, P. G.; Gouterman, M. *J. Mol. Spectrosc.* **1969**, *31*, 1.
(16) Nakamuro, K. *Bull. Chem. Soc. Jpn.* **1982**, *55*, 2697.
(17) Credi, A.; Prodi, L. *Spectrochim. Acta, Part A*, in press.
(18) Lin, X. Q., Kadish, K. M. *Anal. Chem.* **1985**, *57*, 1498.
(19) Naruta, Y.; Sasayama, M.; Sasaki, T. *Angew. Chem., Int. Ed. Engl.* **1994**, *33*, 1839;.
(20) Buchler, J. W. in *The Porphyrins*; Dolphin, D., Ed.; Academic Press: New York, 1978; Vol. 1, p 389 and references therein.
(21) Tabushi, I.; Kugimiya, S.; Kinnaird, M. G.; Sasaki, T. *J. Am. Chem. Soc.* **1985**, *107*, 419.

$[M]^+$. Anal. Calcd for $C_{37}H_{38}N_4O$: C, 80.11; H, 6.90; N, 10.10. Found: C, 80.03; H, 6.83; N, 10.01.

10-Phenyl-(2,18-diethyl-3,7,8,12,13,17-hexamethyl)porphyrin, [(10-Ph)DEHMP)]H_2. (8,12-Diethyl-2,3,7,13,17,18-hexamethyl)-*a*,*c*-biladiene dihybromide (500 mg), benzaldehyde (1 mL), and TsOH (1 g) were dissolved in ethanol and refluxed for 1.5 h. Sodium acetate was added to neutralize the solution, and the solvent was then evaporated under vacuum. The residue was dissolved in CH_2Cl_2 and chromatographed on silica gel (CH_2Cl_2 elution). A red-brown fraction was collected and crystallized from methanol to give [(10-Ph)DEHMP)]H_2 as red-violet crystals (332 mg, 76%). UV−vis: λ_{max} nm, 402, 500, 531, 572, 626. ^{1}H NMR (δ ppm, $CDCl_3$): 10.12 (s, 2H), 9.96 (s, 1H), 8.16 (m, 5H), 4.14 (q, 4H), 3.50 (s, 12H), 2.38 (s, 6H), 1.96 (t, 6H), −3.20 (br s, 2H). FAB-MS: 527 $[M]^+$. Anal. Calcd for $C_{36}H_{38}N_4$: C, 82.09; H, 7.27; N, 10.64. Found: C, 81.95; H, 7.01; N, 10.54.

1-[5-(10,15,20-Triphenylporphyrinyl)]-4-[10-(2,18-diethyl-3,7,8,12,13,17-hexamethylporphyrinyl)]benzene, H_2[*p*-(TPP-DEHMP)]H_2. A 500 mg amount of [(10-Ph-4′-CHO)DEHMP]H_2 (0.78 mmol) was dissolved in 400 mL of propionic acid, and 1.5 mL of benzaldehyde (28.6 mmol) was added. The mixture was gently refluxed during slow addition (8 h) of 2 mL of pyrrole (28.86 mmol) in 50 mL of propionic acid. The reaction was allowed to boil for an additional 16 h, after which it was evaporated under high vacuum. The residue was dissolved in 250 mL of $CHCl_3$ and stirred for 8 h with a 250 mL saturated solution of Na_2CO_3. The organic layer was separated, washed twice with water (100 mL), dried on anhydrous Na_2SO_4, and evaporated to a small volume under vacuum.

The solution was then chromatographed on a silica gel column (80 cm length × 4 cm diameter) using *n*-hexane as a packing solvent. The elution started by using a mixture of $CHCl_3$/*n*-hexane (1:1) to eliminate the TPP product which was generated during the reaction. When the eluate became colorless, the column was eluted with $CHCl_3$. The red fraction obtained was evaporated and chromatographed again on a silica gel column (50 cm length × 2.5 cm diameter) using $CHCl_3$ as eluent in a manner similar to that described above. The fraction containing the dimer was evaporated and recrystallized from $CHCl_3$/*n*-hexane (1:2) to give 99.3 mg (12% yield) of product. ^{1}H NMR (δ ppm, $CDCl_3$): 10.24 (s, 2H), 10.01 (s, 1H), 9.31, 9.12 (each d, 4H), 8.95 (m, 4H), 8.57, 8.39 (each d, 4H), 8.32−8.26 (m, 6H), 7.85−7.75 (m, 9H), 4.08 (q, 4H), 3.52 (s, 12H), 3.04 (s, 6H), 1.92 (t, 6H), −2.58 (s, 2H), −2.99, −3.18 (each br s, 2H). FAB-MS: 1063 $[M]^+$. Anal. Calcd for $C_{74}H_{62}N_8$: C, 83.59; H, 5.88; N, 10.54. Found: C, 83.73; H, 5.68; N, 10.15.

1-[5-(10,15,20-Triphenylporphyrinyl)]-3-[10-(2,18-diethyl-3,7,8,12,13,17-hexamethylporphyrinyl)]benzene, H_2[*m*-(TPP-DEHMP)]-H_2. This dimer was prepared as reported above but starting from [(10-Ph-4′-CHO)DEHMP]H_2. Purification of the compound followed procedures described above for the para isomer. After the second chromatography, an NMR spectrum of the product was shown to contain some impurities. The product was then converted to the bis-zinc derivative (vide infra) and subjected to a column chromatography on a silica gel column (40 cm length × 2 cm diameter) using $CHCl_3$ as eluent. The fraction containing the zinc compound was evaporated to a small volume, CF_3COOH (1 mL) was added under nitrogen, and the solution was stirred for 6 h. The solution was then washed with water, followed by $NaHCO_3$ (sat. sol.), after which it was dried on anhydrous Na_2SO_4 and recrystallized from $CHCl_3$/*n*-hexane (1:2) to give 74.5 mg of product. Yield: 9%. ^{1}H NMR (δ ppm, $CDCl_3$): 10.18 (s, 2H), 9.92 (s, 1H), 9.33, 8.99 (each d, 4H), 8.91 (s, 1H), 8.82 (s, 4H), 8.68, 8.51 (each d, 2H), 8.28−8.12 (m, 6H), 7.82−7.68 (m, 10H), 4.02 (q, 4H), 3.60 (s, 12H), 3.09 (s, 6H), 1.83 (t, 6H), −2.77 (s, 2H) −3.10, −3.29 (each br s, 2H). FAB-MS: 1063 $[M]^+$. Anal. Calcd for $C_{74}H_{62}N_8$: C, 83.59; H, 5.88; N, 10.54. Found: C, 84.02; H, 5.76; N, 10.15.

[(10-Ph)DEHMP]Zn. [(10-Ph)DEHMP)]H_2 (200 mg) was dissolved in 50 mL of $CHCl_3$, and 25 mL of saturated $Zn(CH_3COO)_2$ in methanol was added, after which the mixture was refluxed under nitrogen for 10 min. The solution was diluted with $CHCl_3$ (100 mL) and then washed with water, dried on anhydrous Na_2SO_4, and evaporated to dryness. The residue was recrystallized from $CHCl_3$/methanol to give 209 mg of product. Yield: 93.2%. UV−vis: λ_{max} nm, 410, 539, 575. ^{1}H NMR (δ ppm, $CDCl_3$): 10.11 (s, 2H), 9.94 (s, 1H), 8.12 (m, 5H), 4.16 (q, 4H), 3.53 (s, 12H), 2.35 (s, 6H), 1.98 (t, 6H). FAB-MS: 590 $[M]^+$. Anal. Calcd for $C_{36}H_{36}N_4Zn$: C, 73.28; H, 6.15; N, 9.49. Found: C, 73.11; H, 5.99; N, 9.23.

Zn[*p*-(TPP-DEHMP)]Zn. H_2[*p*-(TPP-DEHMP)]H_2 (50 mg) was dissolved in 100 mL of $CHCl_3$, and 2 mL of saturated Zn $(CH_3COO)_2$ in methanol was added. The mixture was refluxed under nitrogen overnight after which it was washed with water (3 × 50 mL), dried on anhydrous Na_2SO_4, and evaporated to dryness. The residue was chromatographed on silica gel and eluted with a $CHCl_3$/*n*-hexane (1:1). The appropriate fraction was collected, evaporated under reduced pressure and recrystallized from a $CHCl_3$/*n*-hexane (1:2) mixture to give 50 mg of product. Yield: 89.5%. ^{1}H NMR (δ ppm, $CDCl_3$): 9.73 (s, 2H), 9.66 (s, 1H), 9.08, 8.91 (each d, 4H), 8.74 (m, 4H), 8.33, 8.22 (each d, 4H), 8.11 (m, 6H), 7.76 (m, 9H), 3.98 (q, 4H), 3.55, 3.47 (each s, 12H), 2.83 (s, 6H), 1.84 (t, 6H). FAB-MS: 1190 $[M]^+$. Anal. Calcd for $C_{74}H_{58}N_8Zn_2$: C, 74.68; H, 4.91; N, 9.42. Found: C, 74.31; H, 4.80; N, 9.22.

Zn[*m*-(TPP-DEHMP)]Zn. This complex was prepared as reported above for the para isomer but starting from free base H_2[*m*-(TPP-DEHMP)]H_2 (yield 91%). ^{1}H NMR (δ ppm, $CDCl_3$): 9.52 (s, 2H), 9.47 (s, 1H), 9.07, 8.86 (each d, 4H), 8.74 (m, 4H), 8.40, 8.18 (each d, 4 H), 7.98 (m, 6H), 7.63 (m, 9H), 3.82 (q, 4H), 3.38, 3.31 (each s, 12H), 2.74 (s, 6H), 1.70 (t, 6H). FAB-MS: 1190 $[M]^+$. Anal. Calcd for $C_{74}H_{58}N_8Zn_2$: C, 74.68; H, 4.91; N, 9.42. Found: C, 74.25; H, 4.83; N, 9.16.

Acknowledgment. The support of the Robert A. Welch Foundation (K.M.K., Grant E-680) and the Italian CNR (Progetto Finalizzato Chimica Supramolecolare), MURST (40%), and University of Bologna (Funds for Selected Topics) is gratefully acknowledged. We also thank Mr. Alessandro Leoni and Miss Sonia Mini for their technical support.

IC971443F